THE EXPERIMENTS OF SEASONAL PREDICTION USING THE ANALOGY-DYNAMICAL MODEL*

HUANG JIAN-PING (黄建平) AND WANG SHAO-WU (王绍武)
(Department of Geophysics, Peking University, Beijing 100871, PRC)

Received September 29, 1990.

ABSTRACT

From the viewpoint of dynamics, it is convenient to regard the field to be predicted as a small disturbance superposed on the historical analogous field, and thus the statistical technique can be used in combining with the dynamics. Along this line, a coupled atmosphere-earth surface analogy-dynamical model is formulated and applied to making eight seasonal predictions. All of the predictions were initiated from January and have been made from February to August of 1981 to 1988. The experiments of eight-year predictions show certain skill in seasonal prediction, and the skill scores of prediction are greater than those of single statistical analogy forecast.

Keywords: analogy forecast; long-range numerical prediction; statistic-dynamical prediction.

I. INTRODUCTION

The long-range numerical prediction is one of the three main targets in World Climate Research Program (WCRP) and is of common concern to theorists and practicians, but it seems very difficult to attack. Nowadays, the monthly predictions were usually made by running the general circulation model (GCM) in abroad and it required extralarge computer facilities and huge funds. Even so, it could only make monthly prediction in one month ahead and the skill scores can hardly exceed the lowest level which requested operational forecasting. At the same time, the coupled ocean-atmosphere model should be used in making the prediction over one month for considering the change of boundary conditions. It needs a more extralarge computer, and a series of problems in calculation may happen. The seasonal predictions are more difficult than the monthly one. Thus, it is desirable to explore a new approach to making the seasonal prediction. Because the objects of long-range forecasting are the statistical mean quantity, the statistical technique should not be given up, but should be combined with dynamical one in developing dynamical model[1].

The long-range weather forecasting experiences show that the winter circulation and surface conditions such as SST etc. are good predictors of summer circulation

* Project supported by the program of droughts and floods forecast of the Yangtze River and the Yellow River, the National Natural Science Foundation of China and National Post-doctor Science Foundation of China.

and precipitation. Because the evolution of the meteorological fields starting from the similar state, including both initial condition and boundary condition, always keeps such similarity running in a certain period[2], an analogy is often selected from historical data set according to the similarity to the present year. Although the forecasts produced in this way showed some skill, unfortunately, the historical analogous approach imagines the future to be a simple repetition of the history. It limited greatly improving of the skill. Considering from the viewpoint of dynamics, it is convenient to regard the field to be predicted as a small disturbance superposed on the historical analogous field, and thus the statistical technique can be used in combining with the dynamics[3-5]. Along this line, a coupled atmosphere-earth surface analogy-dynamical model is developed and applied to making seasonal prediction. The results are encouraging.

II. Formulation of the Model

The analogy-dynamical model is a coupled atmosphere-earth surface model which includes two parts: the atmosphere and the earth surface. The governing equation for atmosphere is the quasi-geostropic model and the controlling equation for the earth surface is the thermal conduct equation for surface temperature, in which the thermal advection by the current in the oceanic area is taken into account. The interaction between the atmosphere and the surface is accomplished through such physical processes as the surface energy balance[6,7].

Because the evolution of the atmosphere and ocean starting from the similar state, including both initial condition and boundary condition, always keeps such similarity running in a certain period, the evolution of circulation can be regarded as a small disturbance superposed on the historical analogous field. We now divide variables into two components: the basic state and the disturbance state superposed on it, i.e.

$$X = \tilde{X} + \hat{X},$$

where the basic state $\tilde{X}$ is selected from the historical data set according to similarity with initial and its evolution has already been known. $\hat{X}$ is the difference of two analogous year's states and called analogous deviation. Substituting $X=\tilde{X}+\hat{X}$ into the basic equation, and assuming that the basic state satisfies the basic equation, the deviation form of basic equation can be written as follows:

$$\frac{\partial}{\partial t}\nabla^2\hat{\phi} + \frac{1}{f}J(\tilde{\phi},\nabla^2\hat{\phi}) + \frac{1}{f}J(\hat{\phi},\nabla^2\tilde{\phi}) + \frac{1}{f}J(\hat{\phi},\nabla^2\hat{\phi}) + \frac{2\Omega}{a^2}\frac{\partial\hat{\phi}}{\partial\lambda} = f^2\frac{\partial\hat{\omega}}{\partial P} - \alpha\nabla^2\hat{\phi}, \tag{1}$$

$$\frac{\partial}{\partial t}\left(\frac{\partial\hat{\phi}}{\partial P}\right) + \frac{1}{f}J\left(\tilde{\phi},\frac{\partial\hat{\phi}}{\partial P}\right) + \frac{1}{f}J\left(\hat{\phi},\frac{\partial\tilde{\phi}}{\partial P}\right) + \frac{1}{f}J\left(\hat{\phi},\frac{\partial\hat{\phi}}{\partial P}\right) + \sigma_p\hat{\omega} = -\frac{R}{P}\hat{Q}, \tag{2}$$

$$\frac{\partial \hat{T}_s}{\partial t} + \delta\,[J_s(\tilde{\phi}_s, \hat{T}_s) + J_s(\hat{\phi}_s, \tilde{T}_s) + J_s(\hat{\phi}_s, \hat{T}_s)] = K_s \frac{\partial^2 \hat{T}_s}{\partial z^2}, \tag{3}$$

where

$$\nabla^2 = \frac{1}{a^2}\left[\frac{1}{\sin^2\theta}\frac{\partial^2}{\partial\lambda^2} + \frac{1}{\sin\theta}\frac{\partial}{\partial\theta}\sin\theta\frac{\partial}{\partial\theta}\right],$$

$$J(A,B) = \frac{1}{a^2\sin\theta}\left[\frac{\partial A}{\partial\theta}\frac{\partial}{\partial\lambda}\nabla^2 B - \frac{\partial A}{\partial\lambda}\frac{\partial}{\partial\theta}\nabla^2 B\right],$$

$$J_s(A,B) = \frac{\sqrt{2}}{2}\frac{0.0126}{\sqrt{\cos\theta}\,a^2}\left[\left(\frac{\partial A}{\partial\theta} + \frac{1}{\sin\theta}\frac{\partial A}{\partial\lambda}\right)\frac{1}{\sin\theta}\frac{\partial B}{\partial\lambda} - \left(\frac{\partial A}{\partial\theta} - \frac{1}{\sin\theta}\frac{\partial A}{\partial\lambda}\right)\frac{\partial B}{\partial\theta}\right],$$

where $\delta = 1$ for ocean and $\delta = 0$ for land. f is the Coriolis parameter;

$$\sigma_p = \frac{R^2 T}{P^2 g}(r_d - r),$$

the static stability; the deviation of diabatic heating rate

$$\hat{Q} = \frac{\hat{\varepsilon}}{\rho C_p}$$

is

$$\frac{\hat{\varepsilon}}{\rho C_p} = \frac{\hat{\varepsilon}_s}{\rho C_p} + \frac{\hat{\varepsilon}_R}{\rho C_p} + \frac{\hat{\varepsilon}_L}{\rho C_p},$$

where $\hat{\varepsilon}_s$ denotes the deviation of the turbulent heat exchange, the formula is taken as

$$\frac{\hat{\varepsilon}_s}{\rho C_p} = \frac{\partial}{\partial P}K_p\frac{\partial \hat{T}}{\partial P}, \tag{4}$$

where $K_p = \rho^2 g^2 K_T$, K_T is the coefficient heat conductivity. The deviation of the radiation heat exchange $\hat{\varepsilon}_R$ includes solar short-wave radiation which is simply expressed by an empirical formula and atmosphere long-wave radiation which is given by the scheme of Kuo[8]. It can be written as

$$\frac{\hat{\varepsilon}_R}{\rho c_p} = \frac{\bar{I}}{\rho C_p}(1 - C_s\hat{n})(1 - \alpha_s) + \frac{\partial}{\partial P}K_R\rho^2 g^2\frac{\partial \hat{T}}{\partial P} - \frac{\hat{T}}{\tau_R}, \tag{5}$$

where $\bar{I}$ is the solar radiation, C_s the empirical constant, α_s the earth's albedo, the deviation of the amount of cloudiness $\hat{n}$ is taken as[6]

$$\hat{n} = \frac{\hat{\omega}_b}{\tilde{\omega}_0}, \tag{6}$$

where $\tilde{\omega}_0$ is an empirical parameter and

$$\hat{\omega}_b = l_b\nabla^2\hat{\phi}_s/f_0,\quad l_b = \sqrt{\frac{K_T}{2f}}.$$

For the deviation of the heat exchange of condensation $\hat{\varepsilon}_L$, it may be simply param-

eterized[6] as follows:

$$\frac{\hat{\varepsilon}_L}{\rho C_p} = -\frac{L}{C_p}\frac{dq}{dt} \approx \frac{L}{C_p f_0} r \frac{d\ln\tilde{e}_s}{d\tilde{T}} l_b \tilde{q}_s(P)\nabla^2\hat{\phi}_s, \tag{7}$$

where $\hat{\phi}_s$ is the deviation of surface geopotential height. Other symbols are often used in meteorology.

III. Numerical Solution of the Model

1. *The Barotropic Feature of Anomalies*

Firstly, the model atmosphere is divided into three vertical layers in P coordinate, i.e. 300 hPa, 500 hPa and 700 hPa which are indicated by symbols 1, 2, and 3, respectively. Eliminating $\hat{\omega}$ from Eqs. (1) and (2), the geopotential deviation tendency equation is written on these layers. The boundary conditions and vertical differences may be written as

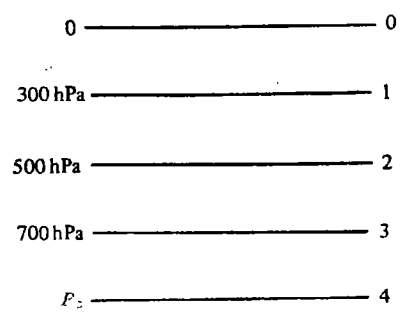

Fig. 1. The vertical structure of the model.

$$P = 0,\ \hat{\omega} = 0,\ \left(\frac{\partial\hat{\phi}}{\partial P}\right)_0 = 0,$$

$$P = P_s,\ \hat{\omega} = 0,\ \left(\frac{\partial\hat{\phi}}{\partial P}\right)_4 = -\frac{R}{P_s}T_s,$$

and

$$\left(\frac{\partial\hat{\phi}}{\partial P}\right)_1 = \frac{1}{\Delta P}(\hat{\phi}_2 - \hat{\phi}_1),$$

$$\left(\frac{\partial\tilde{\phi}}{\partial P}\right)_1 = -\frac{R}{P_1}\tilde{T}_1,$$

$$\left(\frac{\partial\hat{\phi}}{\partial P}\right)_2 = \frac{1}{2\Delta P}(\hat{\phi}_3 - \hat{\phi}_2),\ \left(\frac{\partial\tilde{\phi}}{\partial P}\right)_2 = -\frac{R}{P_2}\tilde{T}_2,$$

$$\left(\frac{\partial\hat{\phi}}{\partial P}\right)_3 = \frac{1}{\Delta P}(\hat{\phi}_3 - \hat{\phi}_2),\ \left(\frac{\partial\tilde{\phi}}{\partial P}\right)_3 = -\frac{R}{P_3}\tilde{T}_3.$$

Because the anomaly field of monthly mean geopotential height has the equivalent barotopic structure[9,10], the deviation of geopotential height in 300 hPa, 700 hPa and surface can be expressed by using the deviation of geopotential height in 500 hPa, i.e.

$$\hat{\phi}_1 = B_1\hat{\phi}_2,\ \hat{\phi}_3 = B_3\hat{\phi}_2,\ \hat{\phi}_4 = \hat{\phi}_s = B_4\hat{\phi}_2,$$

where B_i $(i = 1,3,4)$ is the regression coefficient. So, the vertical difference of deviation term can be written as

$$\left(\frac{\partial\hat{\phi}}{\partial P}\right)_1 = E_1\hat{\phi}_2,\ E_1 = \frac{1}{\Delta P}(1 - B_1),$$

$$\left(\frac{\partial\hat{\phi}}{\partial P}\right)_2 = E_2\hat{\phi}_2,\ E_2 = \frac{1}{2\Delta P}(B_3 - B_1),$$

$$\left(\frac{\partial\hat{\phi}}{\partial P}\right)_3 = E_3\hat{\phi}_2,\ E_3 = \frac{1}{\Delta P}(B_3 - 1).$$

Finally, the geopotential deviation prediction equation of model atmosphere is simplified as the following form:

$$\frac{\partial}{\partial t}(\nabla^2\hat{\phi}_2 - \lambda\hat{\phi}_2) = -\mathscr{L}(\hat{\phi}_2) - \alpha\nabla^2\hat{\phi}_2 + Q_{A1}\hat{\phi}_2 + Q_{A2}\nabla^2\hat{\phi}_2 + Q_{s1}\hat{T}_s, \tag{8}$$

in which

$$\mathscr{L}(\hat{\phi}_2) = \frac{1}{f}[J(\tilde{\phi}_2,\nabla^2\hat{\phi}_2) + J(\hat{\phi}_2,\nabla^2\tilde{\phi}_2) + J(\hat{\phi}_2,\nabla^2\hat{\phi}_2)]$$

$$+ \frac{2\Omega}{a^2}\frac{\partial\hat{\phi}}{\partial\lambda} + J(A_1\tilde{\phi}_3 - A_2\tilde{\phi}_1,\hat{\phi}_2) + J(A_3\tilde{T}_3 - A_4\tilde{T}_4,\hat{\phi}_2),$$

$$\lambda = \frac{f^2}{2\Delta P}\left[\frac{E_1}{\sigma_{p1}} - \frac{E_3}{\sigma_{p3}}\right],$$

$$A_1 = \frac{f}{2\Delta P}\frac{E_3}{\sigma_{p3}}, \quad A_2 = \frac{f}{2\Delta P}\frac{E_1}{\sigma_{p1}},$$

$$A_3 = \frac{f}{2\Delta P}\frac{B_3}{\sigma_{p3}}\frac{R}{P_3}, \quad A_4 = \frac{f}{2\Delta P}\frac{B_1}{\sigma_{p1}}\frac{R}{P_1},$$

$$Q_{A1} = \frac{f^2}{4\Delta P^3}\left[\frac{K_1}{\sigma_{p1}}(E_2 - E_1) - \frac{K_2}{2}\left(\frac{1}{\sigma_{p1}} + \frac{1}{\sigma_{p3}}\right)(E_3 - E_1) - \frac{K_3}{2\sigma_{p3}}E_2\right] + \frac{f^2}{2\Delta p\tau_R}\left[\frac{E_1}{\sigma_{p_1}} - \frac{E_3}{\sigma_{p_3}}\right],$$

$$K_i = K\rho_i^2 g^2, \quad K = K_T + K_R,$$

$$Q_{A2} = \frac{f^2 R\bar{I}}{2\Delta P C_p}\left(\frac{1}{\sigma_{p3}P_3\rho_3} - \frac{1}{\sigma_{p1}P_1\rho_1}\right)(1-\alpha_s)C_s\frac{l_b}{\tilde{\omega}_0}$$

$$+ \frac{f^2 RLrl_bB_4}{2\Delta P C_p f_0}\left[\left(\frac{d\ln\tilde{e}_s}{dT}\tilde{q}_s\right)_1\frac{1}{\sigma_{p1}P_1} - \left(\frac{d\ln\tilde{e}_s}{d\tilde{T}}\tilde{q}_s\right)_3\frac{1}{\sigma_{p3}P_3}\right],$$

$$Q_{s1} = \frac{K_3 f^2 R}{4\Delta P^3 P_s\sigma_{p3}}.$$

2. *The Treatment of Polar Region and the Solution of the Spherical Helmholtz Equation*

Due to the non-uniform of spherical grid, the alternating number is not only too great, but the optimun relaxation factor is difficult to determine and the computational accuracy also cannot be assured by using the alternate over-relaxation method to solve the dispersed spherical Helmholtz equation. In addition, the distance between the grids is shorter and shorter with increasing of latitudes. According to the CFL linear computational stability condition, to require very small time steps in the high latitude region would be impractical for the adopting of long-range numerical prediction model. A new scheme is developed to overcome the two problems at the same time[11]. The principle of this scheme is firstly to solve the spherical Helmholtz equation by using Fourier method and then the short-wave which is less than the critical wavelength is filtered in doing anti-Fourier transform for high latitudes. So, the solution of spherical Helmholtz and the filtering treatment of polar region can proceed at the same time. It is an effective approach to suit the spherical filtering model.

3. *The Solution of Surface Temperature Deviation Equation*

The solution of surface temperature deviation equation requires two vertical boundary conditions. It takes the energy balance deviation equation on the surface and takes $\hat{T}_s$ as zero on the underground depth, i.e.

$$Z = 0,\ \rho_s C_{ps} K_s \left(\frac{\partial \hat{T}_s}{\partial Z}\right) - \rho C_p K_T \left(\frac{\partial \hat{T}}{\partial Z}\right) + \delta \left(\rho L K_T \frac{d \ln \tilde{e}_s}{dT} \frac{\partial \tilde{q}_s}{\partial T}\right) \hat{T}_s$$

$$= -\frac{S_0}{\tilde{\omega}_0 f} l_b B_4 \nabla^2 \phi_2, \tag{9}$$

$$Z = -D,\ \hat{T}_s = 0. \tag{10}$$

By using the time differential form of Eq. (3) and Eq. (11) and Eq. (12), the solution of surface temperaturte deviation for the time step $t + \Delta t$ is of the following analytical form:

$$\hat{T}_{si,j}^{t+\Delta t} = S_1 \hat{T}_{si,j}^{t} + S_2 H_{1i,j}^{t} + S_3 H_{2i,j}^{t} + S_4 \nabla^2 \phi_{2i,j}, \tag{11}$$

in which the time step Δt is taken as 24 h, $H_{1i,j}$ is the thermal advection by oceanic current, $H_{2i,j}$ is the vertical average of the thermal advection in the atmosphere, the right-hand side terms represent the effects of persistency, oceanic thermal advection, atmospheric thermal advection and short-wave radiation deviation adjusted by cloudiness deviation, respectively; S_1, S_2, S_3 and S_4 are corresponding influence coefficients in the following forms:

$$S_1 = D\left(1 + \frac{\rho C_p}{\rho_s C_{ps}} \sqrt{\frac{K_T \tau_R}{K_s \Delta t (\Delta t + \tau_R)}}\right),\ S_2 = -D K_s \Delta t,$$

$$S_3 = -D \frac{\rho C_p K_T \Delta t}{\rho_s C_{ps}} \sqrt{\frac{\tau_R}{K_s (\Delta t + \tau_R)}},\ S_4 = \frac{-D S_0 \sqrt{K_s \Delta t}}{\rho_s C_{ps} K_s \tilde{\omega}_0} \sqrt{\frac{K}{2f}},$$

$$D = \left(1 + \frac{\delta \sqrt{K_s \Delta t}}{D_q} + \frac{\sqrt{K_s \Delta t}}{D_r}\right)^{-1},\ D_q = \frac{\rho_s C_p K_s}{L \rho K r q_s \left(\frac{\partial \ln \tilde{e}_s}{\partial T}\right)^2},$$

$$D_r = \frac{\rho_s C_{ps} K_s}{\rho C_p K} \sqrt{\frac{K \Delta t \tau_R}{\Delta t + \tau_R}},$$

$$H_{1i,j} = \frac{\delta}{K_s} [J(\tilde{\psi}_s, \hat{T}_s) + J(\tilde{\psi}_s, \tilde{T}_s + \hat{T}_s)]_{i,j},$$

$$H_{2i,j} = \frac{1}{K f_0} \left[J\left(\tilde{\phi}_2, \frac{-E_2 P_2}{R} \hat{\phi}_2\right) + J(\hat{\phi}_2, \tilde{T}_2) \right]_{i,j}.$$

4. *Differential Scheme and Main Parameter*

A spherical longitude-latitude grid point screen is used in this model and the grid intervals in the longitudinal and latitudinal directions are 10° and 5°, respectively. The calculation domain is from 5°—90°N. The center difference and Arakawa advection scheme were used in calculating space difference and Jacob term, respectively. A filtering scheme which can filter the amplifying of high frequency perturba-

tions was used in the time integration of atmosphere model[12] and the time step is 4-h increment. The smoothing treatment for deviation of geopotential height and surface temperature are not processed during numerical integration, but the smoothing average for the basic state is treated by using the starting and predicted months. The main parameters of model are taken as: $K_T = 10$ m^2/s, $\tau_R = 3 \times 10^6$s, $K_R = 0.05$ m^2/s^2, $K_t = 10^2$cm^2/s for ocean and 0.005 cm^2/s for land. Because the above parameters are assured by the empirical method and more or less undefined, the parameters Q_{A1}, Q_{A2}, and Q_{s1} which are related to the diabatic heating are corrected by using Chou's inverse approach and the 15-year data set from 1966—1980 is used for inversing.

IV. The Seasonal Prediction Experiments

Eight seasonal predictions have been carried out by using the analogy-dynamical model from 1981 to 1988. All of the predictions have been initiated from January and predicted from February to August. The predicted anomaly is given by adding the deviation field predicted by the model to the anomaly of the basic state at the corresponding time. Numerical integrations are run month by month. One month prediction is the average from 1 to 30 days. For inspecting the forecast capacity of the model, the model predicted 500 hPa and surface temperature monthly anomalies are compared with the observed one and the skill scores are also compared with statistical analogy forecasts. The evaluating approach is to add up the percent of the points in which the sign of anomaly was correctly predicted (the total number of grid points is 540).

1. *The Predicted Skill of Model*

The skill scores for both 500 hPa (ϕ') and surface temperature (T_s') monthly anomalies from February to August of 1981—1988 are shown in Table 1, from which it can be found that the skill scores of this model are greater than the random forecasts (50%). The highest level for 500 hPa and surface temperature reach 70% and 72%, respectively. All of the annual mean skill scores from February to August are also better than random forecasts, the highest level for 500 hPa and surface temperature reach 59% and 58%, respectively. The mean skill scores of eight predictions for 500 hPa and surface temperature reach 56.8% and 55.4%, respectively. The stability skill scores with time and the greater values of scores show certain skill of the model.

The variation of the skill with latitudes is shown in Fig. 2. The average is from February to August of 1981—1988. It is found that the skill is better at low latitudes and polar regions than at mid-high latitudes, i.e. the skill of 25°N reaches 61%.

The predicted and observed anomalous fields of 500 hPa geopotential height for July 1983 are shown in Fig. 3. Comparing Fig. 3(a) with Fig. 3(b), it is found that the predicted field is close to the observed one. It is shown that the forecasts by this model are acceptable.

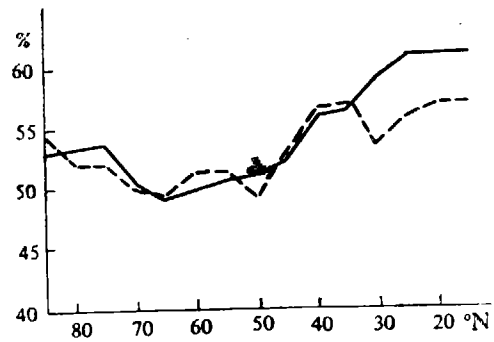

Fig. 2. The variation of the mean skill with latitudes. Solid line represents the anomaly of 500 hPa, dashed line the anomaly of surface temperature.

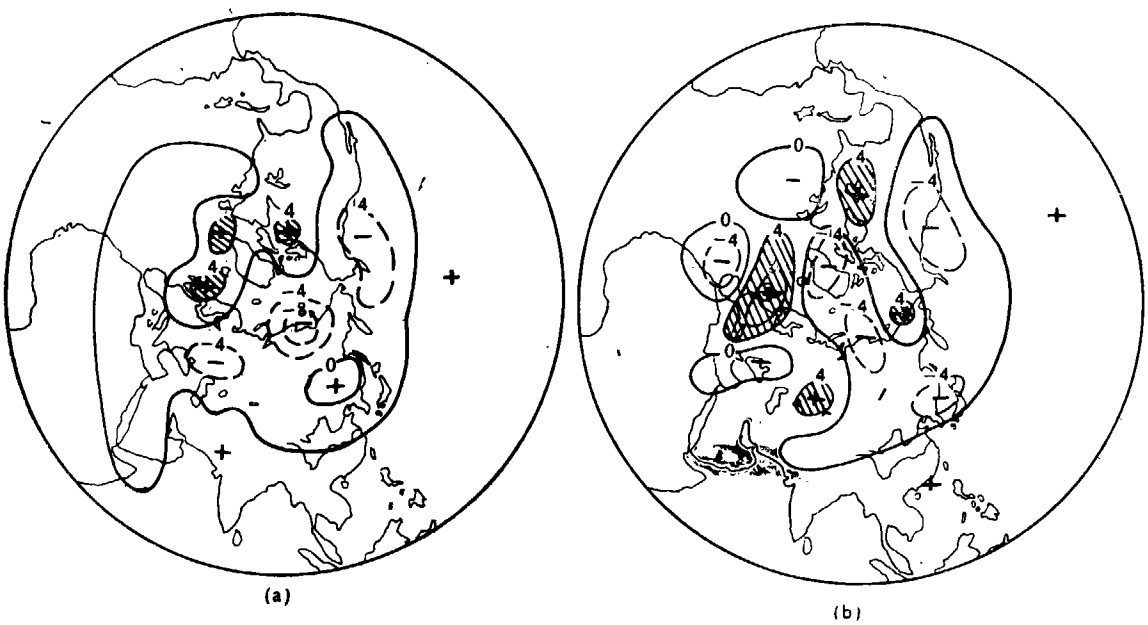

Fig. 3. Predicted (a) and observed (b) 500 hPa anomaly field for July 1983.

2. *Comparing the Model Predictions With Those Made From Analogy*

To inspect the skill of model prediction further, the results of model predicted are compared with single analogy forecast at the corresponding region and time. In fact, the analogy forecast was the anomaly field of the basic state, which was selected from the historical data set according to the similarity in winter and took the evolution of the historical analogous field as the forecasted field. The mean skill of the prediction by this model and that by using single analogy are shown in Fig. 5. Comparing the two forecasts, it can be found that the prediction by this model is much better than single analogy forecast, especially in summer months. It follows that when the dynamical process of analogous evolution of circulation anomaly is taken

into consideration, the prediction skill is better improved than that based on statistical analogy only.

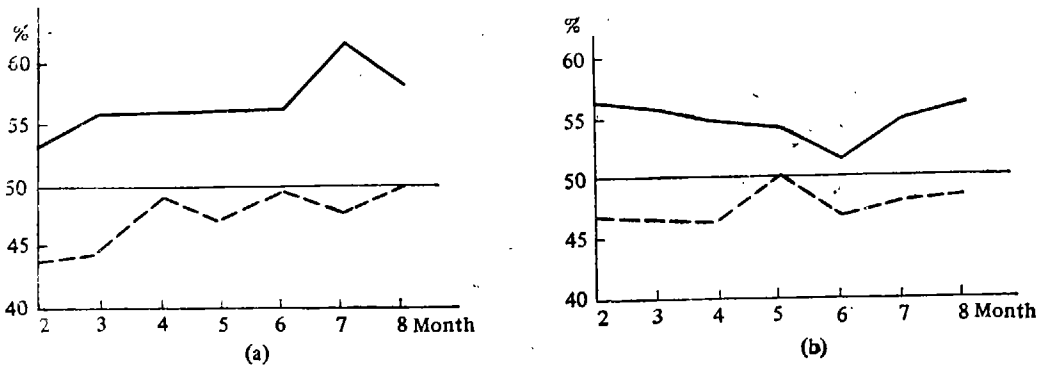

Fig. 4. The mean skill of model (solid line) and analogy (dashed line).

Table 1

The Skill Scores of ϕ' and T'_S Prediction by This Model (ϕ'), the 500 hPa Anomaly; T'_S, the Surface Temperature Anomaly

Term \ Month / Year		Feb.	Mar.	Apr.	May	Jun.	Jul.	Aug.	Mean
1981	ϕ'	53	53	48	60	48	53	60	53.6
	T'_S	59	51	48	58	44	47	58	52.1
1982	ϕ'	60	48	53	54	55	57	58	55.0
	T'_S	55	53	50	51	48	54	57	52.6
1983	ϕ'	52	56	59	53	59	70	62	58.7
	T'_S	61	58	59	57	59	56	59	58.4
1984	ϕ'	55	50	51	54	65	69	65	58.4
	T'_S	54	60	49	61	55	62	55	56.6
1985	ϕ'	48	62	62	65	56	53	52	56.9
	T'_S	50	57	57	50	55	50	53	53.2
1986	ϕ'	51	58	65	64	59	60	56	59.0
	T'_S	58	58	55	53	50	61	55	55.7
1987	ϕ'	62	61	55	48	57	65	55	57.6
	T'_S	72	60	61	53	47	51	56	57.1
1988	ϕ'	46	58	55	51	50	69	57	55.1
	T'_S	50	56	57	51	53	58	57	54.6

V. Conclusions

These results of seasonal prediction experiments show that the analogy-dynamical model has a certain skill in the seasonal prediction and the skill scores of prediction are greater than those of single analogy forecasts. It can remedy partially the defects of model with information provided by the historical data set and the statistical technique can be used in combining with dynamics. These results of prediction experiments are encouraging.

To be sure, these experiments are preliminary, the model will be further improved by more experiments, i.e. the parameterization of diabatic and land processes are required to improve as well. In addition, the selection of the basic state is also important for improving the prediction skill. The authors believe that the analogy-dynamical model, after further improvement, will be of use for operational monthly and seasonal weather predictions.

The authors wish to express their gratitude to Prof. Chou Ji-fan for helpful discussion.

References

[1] 丑纪范，长期数值天气预报，气象出版社，1986.
[2] 王绍武，长期天气预报基础，上海科学技术出版社，1987.
[3] 丑纪范，中长期水文气象预报文集，水利电力出版社，1979, pp. 216—221.
[4] 黄建平等，中国科学B辑，1989, 9:1001.
[5] 邱宗践等，大气科学，14(1989), 22.
[6] 巢纪平等，中国科学，1977, 2:162.
[7] Lin Benda et al., *Acta Oceanologica Sinica*, 7(1988), 369.
[8] Kuo, H. L., *Pure and Appl. Geophy.*, 109(1973), 1870.
[9] 黄建平等，长期天气预报文集，气象出版社，1990, pp. 57—66.
[10] 黄建平等，高原气象，7(1988), 264.
[11] 衣育红，北京大学学报，1990, 5: 627.
[12] 张玉玲等，数值天气预报，科学出版社，1986.